ANTIBACTERIAL EFFECT OF TRANSITION METAL BASED BIOACTIVE NANOCOMPOSITE COATINGS ON TITANIUM IMPLANTS

Priyanka S Shaji, Suja Mathai[*],

PG and Research Department of Chemistry, Mar Ivanios College (Autonomous), Thituvananthapuram-695015, Kerala, India.

Corresponding Author:** **Dr. Suja Mathai

sujamathaikunnath@gmail.com

ABSTRACT

For years, researchers' attentions have focused on the use of Ti as implant materials because of their outstanding biocompatibility, high corrosion resistance and great fatigue. Ti, however, lacks mechanical strength when it is pure. Also, antibacterial activity, bioactivity and biocompatibility of Ti metals should be improved in order to utilize them as biomaterials. Niobium pentoxide (Nb_2O_5) coatings have shown enormous potential for usage in implants due to their superior physiochemical qualities to facilitate bone regeneration and cell proliferation. Incorporating silver (Ag) into Nb_2O_5 coating is an excellent way to impart the coatings antibacterial properties. In this study, we employed pulsed electrochemical deposition to co-deposit Nb_2O_5 and Ag simultaneously to uniformly distributed Ag particles in the coatings on Ti substrate. The Nb_2O_5-Ag nanocomposite coatings were chosen and subjected for in vitro study in Kokubo's 1.5 simulated body fluid after alkaline treatment. The coatings were subjected to physico-chemical characterization, electrochemical evaluation, surface morphological and topography analyses. The characterization technique revealed that apatite was grown on the surface of Nb_2O_5-Ag nanocomposite coating system. The in vitro antibacterial and in vitro cytotoxicity tests was performed at different concentrations which proves the significant effect in antibacterial effect and cellular response with no toxicity respectively. Antibacterial assays determined that treatment with nanocomposite coating at concentrations of 0.62 to 5 µg/mL induced a decay in the growth of both Gram-negative and Gram-positive bacteria. The highest zone of inhibition was observed for *Staphylococcus aureus* and *Escherichia coli* respectively. The Nb_2O_5-Ag nanocomposite coating on Ti metals could efficiently act as a barrier for the probable release of metal ions from the substrate and favoring further biogrowth on implantation for its long-term applications without any toxicity and excellent antibacterial properties.

Keywords: Niobium pentoxide, pulsed deposition method, antibacterial, sodium niobite, cytotoxicity, nanocomposites.

INTRODUCTION

Titanium has excellent mechanical strength, good corrosion resistance and biocompatibility and have been widely used for producing implants such as hip joint prostheses, knee joint prostheses and dental implants [1, 2]. Titanium implants with bioactive coatings are commonly used in clinics because they are able to generate good osteointegration with bone tissue for titanium implants [3]. Although, these coatings osteoconductive, the problems of bacterial infections related to biomedical implants persist [4, 5]. The bacterial infections on titanium implants are usually difficult to treat and may lead to necessary medical antibiotic therapies, and even implant removal [6]. It is imperative to develop coatings that provide excellent antibacterial activity and osteointegration simultaneously [7].

Recently, oxides of niobium have governed increased attention due to their potential for biological applications with excellent biocompatibility [8]. It was also demonstrated that the oxide of niobium shows cell proliferation, mitochondrial activity and cell volume [9]. Silver has long been known to have strong inhibitory and bactericidal effects as well as a broad spectrum of antimicrobial activities [10-12]. It also exhibits high thermal stability and low toxicity towards mammalian cells [13 ,14]. Electrochemical deposition method (ECD) becomes a popular coating method owing to its ease of processing control, variability of the coating composition and suitability for complex implant geometries [15,16]. Zhitomirsky *et al.* found cathodic electrolytic deposition of niobium oxide films on metal substrates [17]. Liu *et al*. produced composite coatings using ECD by adding silver powder in the electrolyte [18]. ECD is one of the promising methods to prepare silver- loaded niobium oxide coatings.

The present study was based on a thin electrodeposited layer of niobium oxide from a well-designed aqueous acidic electrolytic solution containing niobium precursor ($NbCl_5$), where silver ions are added. Also, this study focuses on investigating the effects of silver doped niobium oxide thin film coatings on the antibacterial properties and biocompatibility of the coatings by pulsed electrochemical deposition (PED) which have potential applications in bone implant.

MATERIALS AND METHODS

Materials

Commercially available pure Ti specimens (Grade T3160) of area 2 × 1 cm^2 and 1 mm thickness were used as the substrate for the coating were purchased from Sigma Aldrich (Germany). They were mechanically polished using 36- grit SiC paper, rinsed with water followed by ethanol and then with acetone for 15 min each. Niobium (V) chloride, $NbCl_5$, 99.9%, Sigma Aldrich), Nano silver nitrate powder ($AgNO_3$, 99.9%, Merk), Isopropyl alcohol (IPA, 99.9%, Sigma Aldrich) were used as the raw materials. Calcium nitrate tetrahydrate, $Ca(NO_3)_2.4H_2O$ (98%, Spectrum), ammonium dihydrogen orthophosphate, $NH_4H_2PO_4$ (99%, Rankem), sodium hydrogen carbonate (purified), $NaHCO_3$ (99%, Merk), dipotassium hydrogen orthophosphate, K_2HPO_4 (99.9%, Fisher Scientific), magnesium chloride, $MgCl_2.6H_2O$ (98%, Nice), calcium chloride dehydrate, $CaCl_2.2H_2O$ (97%, Fisher Scientific), sodium sulphate anhydrous A.R., Na_2SO_4 (98%, Merk), tris buffer A.R., $(CH_2OH)_3CNH_2$ (99%, Spectrum), sodium hydroxide pellets A.R. (99%, SRL) were used in this study.

Pulsed Electrochemical Deposition (PED) Method

The Ti substrates were first etched for an hour using a solution containing 4 ml conc. HNO_3 (68%) and 4 ml H_2O_2 (30%) in order to remove oxide and increase the substrates' roughness for improved adherence. Following the etching procedure, the specimens were cleaned with distilled water and allowed to air dry for 30 minutes. The electrodeposition carried out in a three-electrochemical cell, the etched strip act as working electrode i.e., cathode and the platinum (Pt) mesh act as counter electrode (anode) and a standard calomel electrode act as reference electrode. After pretreatment, the PED was carried out in an electrolytic solution containing an aqueous acidic solution. Nb_2O_5 thin films are electrodeposited onto Ti substrate from an aqueous solution containing niobium pentachloride ($NbCl_5$) solution. 185 mg $NbCl_5$ was dissolved in 40 mL isopropyl alcohol into 60 mL H_2O_2, resulting in a clear colloidal solution. The Nb_2O_5-Ag nanocomposite coatings were prepared by adding nano silver nitrate powder into the electrolyte. The solution was kept at room temperature for 3 h before electrodeposition [19]. The deposition was carried out at a cathodic potential of -1.5, -2 and -2.5V at current density of 1 mA for 30 mins. After deposition, the Ti substrate with coatings were dried at room temperature and then cooled. The prepared coatings were chosen for alkaline treatment in 5M NaOH at 60^oC for 24

hours followed by biomimetic growth in Kukubo's 1.5 Simulated Body Fluid (SBF) for 14 days at 36.5^{o}C.

Electrochemical investigation

Electrochemical impedance spectroscopy (EIS) and cyclic voltammetry (CV) in a 0.9% NaCl solution were used to examine the electrochemical behavior of nanocomposite coatings that had been produced on Ti. In a typical three electrode cell, the electrochemical studies were carried out. Ti was used as the working electrode for all measurements, with the saturated calomel electrode (SCE) and the platinum (Pt) electrode working as the reference and counter electrodes, respectively. All electrochemical studies were performed in electrochemical workstation using Metrohm Autolab PGSTAT204 instrument. The EIS measurements were performed in the potential range of 0.1 V to 1.5 V. The obtained data was recorded by the use of internally available software (Autolab), and each experiment was repeated three times to check reproducibility. The solution was kept unstirred and CV was recorded in the potential range -1.0V to 1.0V at a scan rate of 0.01V s^{-1}.

Evaluation of in vitro for bioactivity

In vitro mineralization of the developed coatings can be studied in 1.5 Kukubo's simulated body fluid (SBF) for 20 days at 36.5^{0}C. The specimens were then soaked in 20 ml of an acellular simulated body fluid (1.5 SBF) of composition Na^{+}: 213.0, K^{+}: 7.5, Mg^{2+}: 2.3, Ca^{2+}: 3.8, Cl^{-}: 221.7, HCO_3^{-}: 221.7, HPO_4^{2-} : 6.3, SO_4^{2-}: 0.8 mmol/L at 36.5^{0}C and pH 7.4 [20,21]. The SBF solution was prepared by dissolving the required amount of reagent-grade chemicals of NaCl, $NaHCO_3$, KCl, K_2HPO_4. $3H_2O$, $MgCl_2$. $6H_2O$, 1.0 M HCl, $CaCl_2$, Na_2SO_4 in distilled water and buffered to pH using a solution of tris-hydroxylmethyl aminomethane ($(CH_2OH)_3CNH_2$). The surface potential change during biomimetic growth was monitored by open circuit potential (OCP), with reference to a saturated calomel electrode using a digital multimeter (SYSTRONICS 437T). The crystallinity, chemical composition, microstructural morphology and surface roughness studies of the coatings before and after the biomimetic study was analyzed microscopically and spectroscopically. To determine the phase purity of the synthesized coating materials, X-ray diffraction (XRD, Bruker D8 ADVANCE with DAVINCI design) was performed. Phase identification was carried out by comparing the peak positions of the diffraction patterns with ICDD (JCPDS) standards. The chemical functional groups were

characterized by Fourier transform infrared spectroscopy (FTIR, Thermoscientific Nicolet iS50). FTIR spectra were recorded from 400 to 4000 cm^{-1}. The surface morphological analyses along with compositional elemental analyses of the coating were carried out using a scanning electron microscope (SEM) and) energy dispersive spectroscopy (EDS), Carl Zeiss EVO 18 Research. The surface roughness morphology of the coatings was determined by using atomic force microscopy (AFM), Nanosurf Flex-ANA instrument.

In vitro antibacterial test

The synthesized Nb_2O_5-Ag nanocomposite coatings was studied by the standard disc diffusion method as described in European pharmacopeia with slight modification was used for antibacterial testing [22]. Bacterial stock cultures of Gram-positive bacteria (*Bacillus subtilis* MNN 2111 and *Staphylococcus aureus* MTCC 96), and Gram-negative bacteria (*Pseudomonas aeruginosa* ATCC 27853 and *Escherichia coli* MTCC 443) maintained at Biovent Innovations Pvt Ltd, was used for the test. 0.625, 1.25, 2.5 and 5 mg/mL concentration of the sample was used for the screening of the antibacterial activity. 0.125 mg/mL of Streptomycin was used as the standard drug (positive control) and 0.05% DMSO was used as negative control. Sterile Muller Hinton agar (MHA) plates were used for the test. 100 µl of the pure cultures of test strains were swabbed uniformly using a sterile swab on the surface of MHA plate to obtain an even inoculum. The plates were allowed to dry for 5 minutes and different concentration of the sample, DMSO and standard drug containing disk were placed on the MHA plates. The antibacterial activity was observed after incubating the plates for 24 hours at 37^0C and the zone of inhibition surrounding the well were noted in mm [23].

In vitro cytotoxicity test

In vitro bioassay was conducted and determined by the Biovent Innovations Pvt Ltd, Department of Biotechnology, University of Kerala. L929 (ISO certified normal fibroblastic cell line) was selected for MTT analysis. The cell-lines were purchased from National Centre for Cell Culture (NCCS), Pune, India. The cell lines were maintained in T-25 tissue culture flask with DMEM supplemented with 10% FBS and antibiotic solution containing penicillin (100 µg/mL), streptomycin (100 µg/mL) and amphoteracin B (2.5 µg/mL). Cultured cell lines were kept at 37ºC in a humidified 5% CO_2 incubator (NBS Eppendorf, Germany). Confluent flasks were trypsinized with 500 µL of 0.025% trypsin in PBS with 0.5 mM EDTA solution and centrifuged

at 1500 rpm for 5 min at room temperature. The supernatant was discarded and the pellet was resuspended in required quantity of DMEM for subculturing / freezing / seeding in well-plates for assay studies. Five different concentrations (6.25 µg/mL, 12.5 µg/mL, 25 µg/mL, 50 µg/mL and 100 µg/mL) were made from the stock of 1 µg/mL DMSO (0.5%). 5 mg MTT powder was dissolved in 1 mL sterile PBS. 100 µL of 20% MTT solution (20 µL MTT and 80 µL DMEM) was used. The prepared MTT was kept in dark [24]. 100 µL of media (DMEM) containing 5000 cells/wells was added to each well of a 96 well ELISA plate. Outermost wells of the 96 well ELISA plate was filled with PBS buffer in order to prevent the evaporation of the sample. The plates were kept overnight for 24 h incubation at 37˚C in a humidified 5% CO_2 incubator. After incubation, plates were taken out and the spent media was discarded. 100 µL of sample at different concentrations were added to corresponding wells. The negative control wells were loaded with 100 µL of DMEM with 0.5% DMSO and in the positive control wells 100 µL of standard drug doxorubicin were added. Samples were assayed in triplicates. After 24 h of incubation, the media was removed and the wells were washed with 100 µl PBS buffer. 100 µL of MTT dye was added after the removal of PBS. Incubation was carried out for 2 h in dark. 100 µL of MTT lysis buffer (20% SDS in 50% dimethyl formamide) was added and incubated for 4 h in dark. The absorbance was measured at 570 nm using microplate reader (Thermoscientific Multiskan Go version 1.00.40) and the percentage viability was calculated using formula.

$$\% \text{ Viability} = \frac{\text{OD of the test}}{\text{OD of the control}} \text{x } 100$$

The IC_{50} value is the half maximal inhibitory concentration of the sample. The IC_{50} values were calculated using the equation for slope (y = mx + C) obtained by plotting the average absorbance of the different concentrations of the test sample (6.25-100 µg/mL), where OD is the optical density.

RESULTS AND DISCUSSION

Physio-chemical characterization

X-ray diffraction Spectroscopy (XRD)

XRD patterns of the surfaces of Ti samples of Nb_2O_5-Ag nanocomposite coating treated in 5M NaOH is shown in Figure 1(a). The peaks observed at $2\theta = 38.49^o$, 44.46^o, 64.88^o, and 77.62^o are

assigned to (111), (200), (220), and (311) lattice planes of fcc Ag nanoparticles (JCPDF card no. 04-0783) respectively [25]. In Figure 1(a), the peak at 54.337^o is due to the formation of Na_2O after alkaline treatment which improves the crystallinity of coating. Figure 1(b) shows XRD patterns of Nb_2O_5-Ag nanocomposite coating on Ti treated in 5M NaOH and after immersion in SBF solution for 14 days at 36.5^{o}C. The broad peak located at 2θ= 40.113^o is due to formation of Ag nanoparticles. The characteristic peaks at 52.942^o and 54.268^o is due to the formation of Na_2O after treatment with NaOH, results in orthorhombic crystal structure of sodium niobate ($NaNbO_3$) which were in good agreement with the JCPDS 33-1270 [26]. The coating shows characteristic peaks at 31.667^o, 36.036^o and 70.595^o indicates crystalline nature of apatite after immersion in SBF for 14 days. These observed characteristic peaks are attributed to the formation of crystalline nature of sodium niobate-silver ($NaNbO_3$-Ag) nanocomposite coating treated with 5 M NaOH and after immersion in SBF. The results indicate that the crystalline nature of coatings with orthorhombic structures are effective for apatite nucleation. It has been reported that the orthorhombic niobium oxide is more negatively charged and apatite deposition in body environment is assumed to be preferentially induced by negative functional groups [27]. The orthorhombic niobium oxide provides more favorable condition for the apatite nucleation in SBF. The developed Nb_2O_5-Ag nanocomposite coating is treated 5M NaOH at 60^{o}C for 24 hours to form sodium niobate on its surface which is given by the equation:

$$Nb_2O_5 + 2NaOH \rightarrow NaNbO_3 + H_2O$$

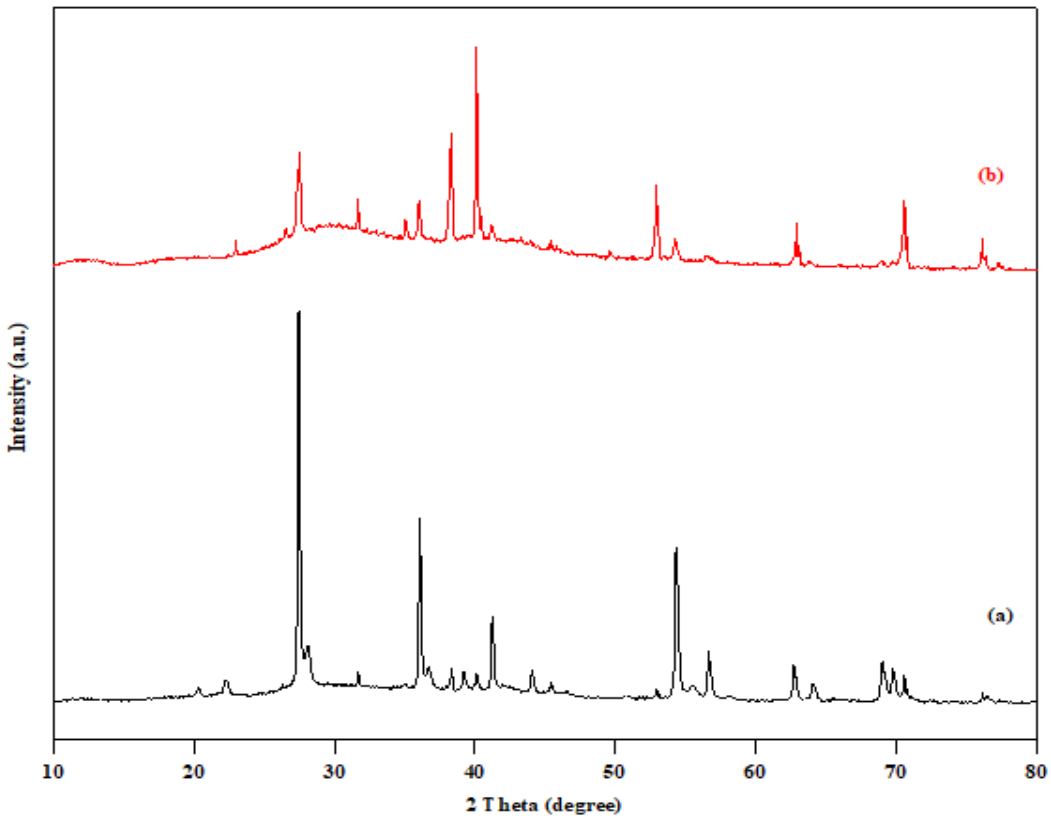

Figure 1: XRD patterns of (a) Nb_2O_5-Ag nanocomposite coating treated with 5M NaOH, and (b) Nb_2O_5-Ag nanocomposite coating on Ti substrate treated with NaOH and after immersion in SBF for 14 days at 36.5°C.

Fourier transform infrared (FTIR) spectroscopy

The FTIR spectra of Nb_2O_5-Ag nanocomposite coating on Ti substrate was shown in figure 2. Figure 2(a) represents the FTIR spectra of Nb_2O_5-Ag nanocomposite coating treated in SBF, where absorption bands ascribed to Nb-OH or to hydrated water were detected at 3453.77 cm^{-1} and 3049.24 cm^{-1}. A peak at 1685.30 and 1443.64 cm^{-1} exhibited silver nanoparticles [28]. The band at 1058.05 cm^{-1} is due to the stretching vibration bonds of sodium hydroxyl group. The analysis revealed the structural integrity of niobium pentoxide changed to sodium niobate ($NaNbO_3$-Ag). Figure 2(b) represents the FTIR Spectra of sodium niobate ($NaNbO_3$) where absorption bands ascribed to Nb-OH or to hydrated water were detected at 3455.27 cm^{-1} and 3036.21 cm^{-1}. The band appeared at 560.84 cm^{-1} represents the Nb-O bond formation [28]. The band at 1685.32 cm^{-1} is due to the presence of silver nanoparticles in the coating. The band at 1449.72 cm^{-1} and 1057.73 cm^{-1} is due to the stretching vibration bonds of sodium hydroxyl

group and carbonate ions of apatite phase. The band appeared at 483.25 cm^{-1}, 471.38 cm^{-1}, 460.81 cm^{-1} and 413.53 cm^{-1} represents the phosphate ion group [29].

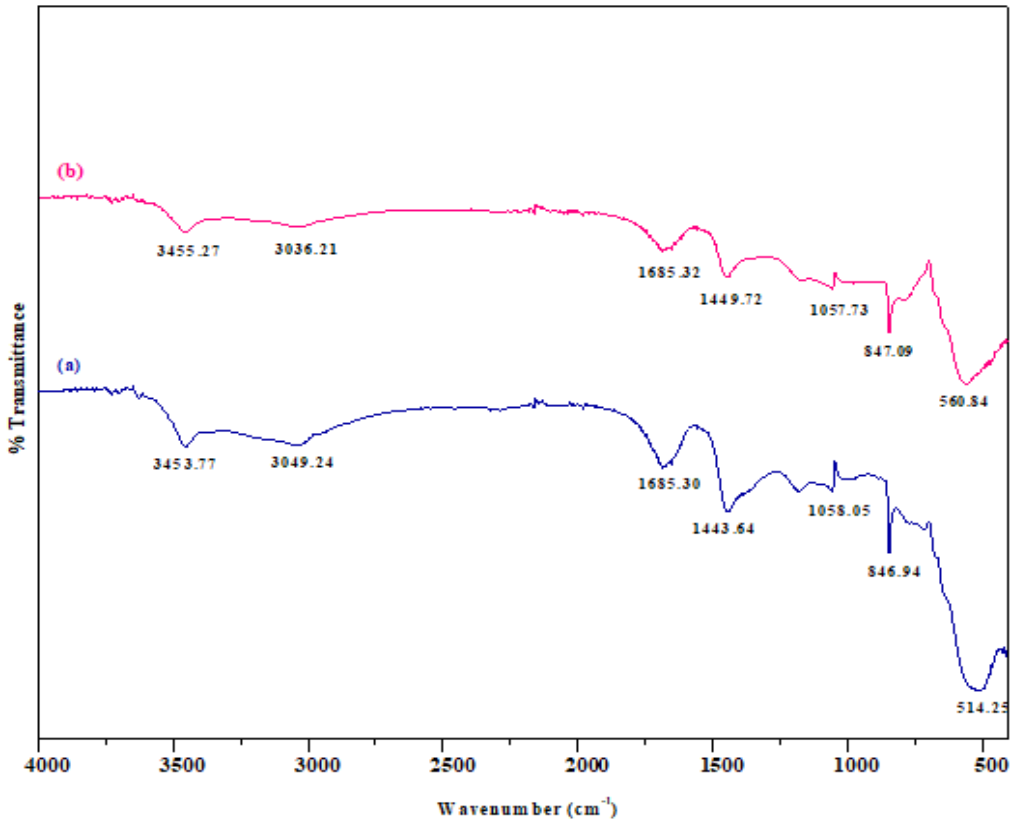

Figure 2: FTIR image of (a) Nb_2O_5-Ag nanocomposite coating treated with 5M NaOH, and (b) Nb_2O_5-Ag nanocomposite coating on Ti substrate treated with NaOH and after immersion in SBF for 14 days at 36.5^oC.

Electrochemical investigation

Electrochemical impedance spectroscopy (EIS)

EIS analyses is used for the determination of coatings adhesion strength and corrosion. EIS of the bode plots of the Nb_2O_5-Ag nanocomposite coatings on Ti in 0.9% NaCl treated is shown in Figure 3. In figure 3(a) and (b), on examining the bode plot it was found the R_{ct} (charge transfer resistance) values to be decreased with increase in the C_{dl} (double layer capacitance) values. An

increase in impedance at high frequencies exhibits more adhesion strength suggesting a depletion of Ca^{2+} and PO_4^{3-} ions in the solution, likely due to the ionic exchanged involved in the formation of the bone-like apatite [30]. In the bode plot of the Nb_2O_5-Ag coated Ti specimens, the inductance was recorded at the end of the semi-circle of the high frequency region. The higher R_{ct} and C_{dl} values obtained for the Nb_2O_5-Ag nanocomposite coatings suggest that the outer layer is highly porous is nature and high resistance after immersion in SBF. Porous nature of the coating could favor osseointegration in body environment which may be the reason for high biomimetic growth rate.

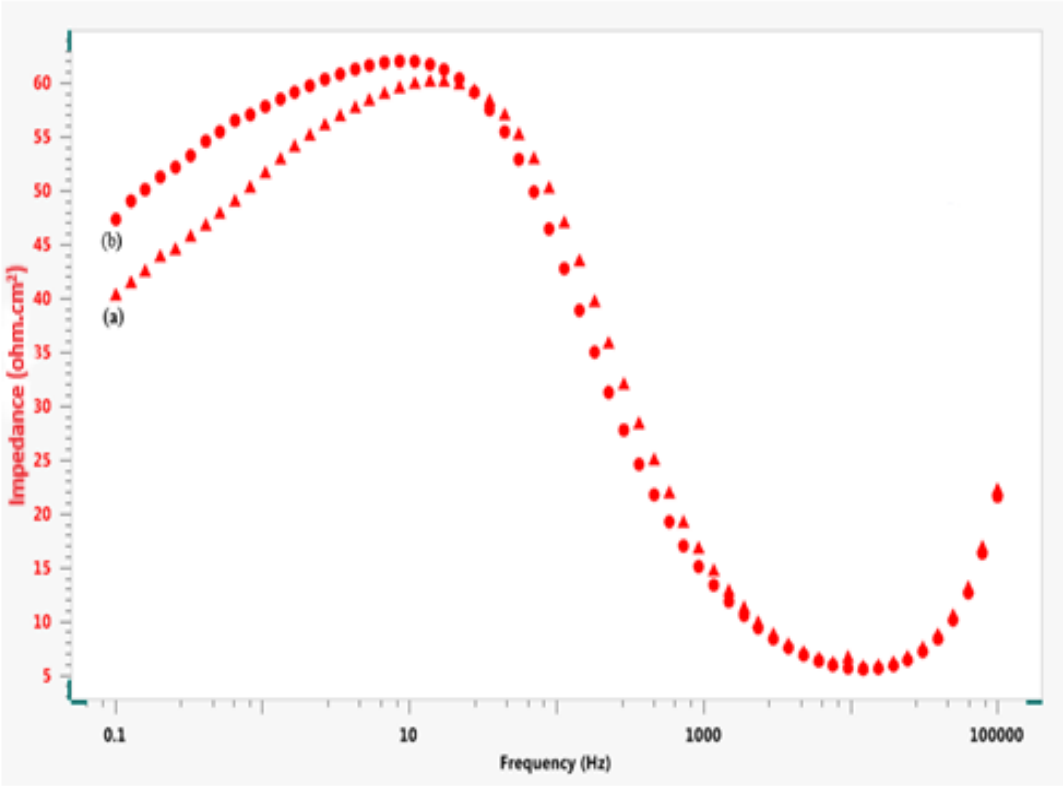

Figure 3: Electrochemical impedance spectroscopy (EIS) of (a) bode plot of Nb_2O5-Ag nanocomposite coating treated in 5M NaOH and (b) bode plot of Nb_2O_5-Ag Ti substrate treated in 5M NaOH and after immersion in SBF at 36.5^oC on Ti substrate.

Table 1: The electrochemical impedance parameters.

S. no.	Samples	R_{ct} (Ω)	C_{dl} (F)
1	Nb_2O_5-Ag nanocomposite coating on Ti substrate treated with 5M NaOH	16,028	0.82 e^{-6}
2	Nb_2O_5-Ag nanocomposite coating on Ti substrate treated with 5M NaOH and after immersion in SBF	18,494	1.09 e^{-5}

Cyclic voltammetry (CV)

Cyclic voltammograms is a type of potentiodynamic measurement which is used to predict electrochemical stability and corrosion resistance of the Nb_2O_5-Ag nanocomposite coatings treated on Ti substrate. Figure 4 represents the cyclic voltammogram of the Nb_2O_5-Ag nanocomposite coating on Ti substrate that was performed in a typical three- electrode electrochemical cell over a range of -1.0 to 1.0 V, in a solution of 0.9% NaCl solution. The Nb_2O_5-Ag nanocomposite coating on Ti substrate treated with 5M NaOH observed in figure 4(a) shows that the electrochemical reaction of electroactive species in the electrolytic solution started to occur at a potential of about -0.1 V. A drastic increase of current density from -0.004 to -0.009 A was observed from a potential ranging from -1.0 V to -0.25 V corresponding to the mass transport-controlled process. Figure 4(b) shows the Nb_2O_5-Ag nanocomposite coating on Ti substrate treated with 5M NaOH and after immersion in SBF for 14 days at 36.5^{o}C. A sudden rise in current density from -0.004 to -0.00098 A between a potential of -1.0 V to 1.0 V results in the deposition of Ca^{2+} and PO_4^{3-} in the Nb_2O_5-Ag nanocomposite coating matrix after biomimetic growth. The evolution of hydrogen was the dominant reaction which happens at a potential > 0.5 V with a lot of bubbles were observed at the Ti surface during scanning. From these findings, it can be concluded that the desirable potential range for good adhesion strength nanocomposite coatings on Ti substrate without the interference of hydrogen evolution in between -0.9 V to 0.5 V. The Nb_2O_5-Ag nanocomposite coatings treated with 5M NaOH and after immersion in SBF for 14 days could withstand high current density and there was no

detachment from the Ti substrate suggest high adhesion strength. This was attributed to the high mechanical stability of the nanocomposite in the biological fluids.

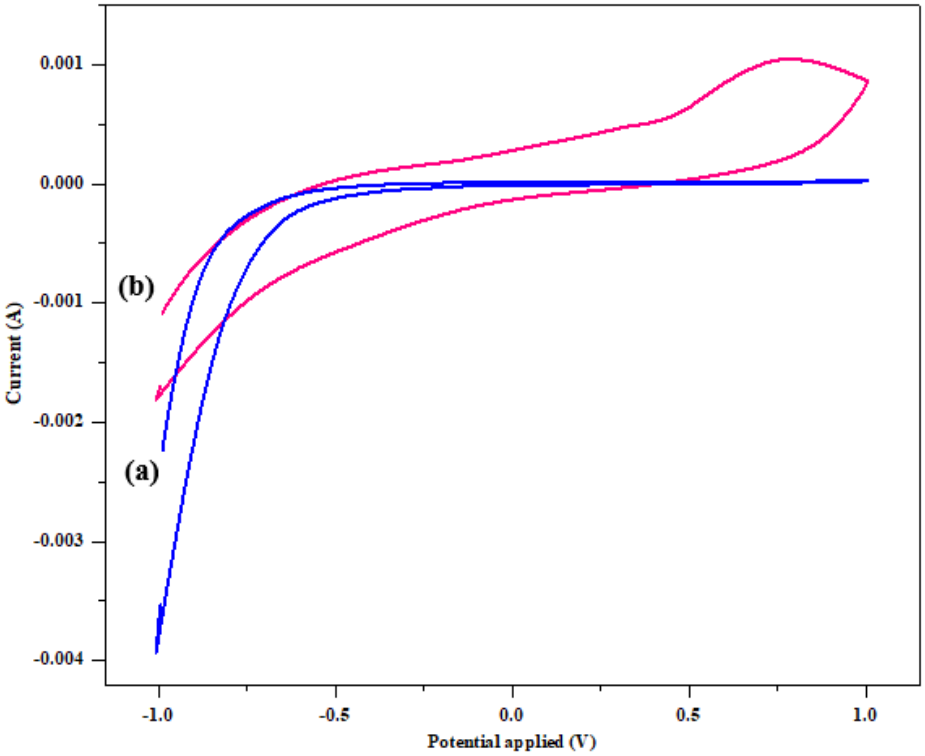

Figure 4: Cyclic voltammograms (a) Nb_2O_5-Ag nanocomposite coating treated with 5M NaOH and (b) Nb_2O_5-Ag nanocomposite coating treated in 5M NaOH and during immersion in SBF at 36.5^{o}C (pH: 7.4).

Evaluation of in vitro mineralization for bioactivity

Scanning electron microscopy-Energy dispersive spectroscopy (SEM-EDS)

SEM micrograph and associated EDS pattern of the Nb_2O_5-Ag nanocomposite coating treated with 5M NaOH and Nb_2O_5-Ag nanocomposite coating treated with 5M NaOH and after immersion in SBF for 14 days on etched Ti substrate are presented in Figure 5. The Nb_2O_5-Ag nanocomposite coating on Ti treated with 5M NaOH has a white precipitate-like small crystallites which may be due to the presence of silver nanoparticles are shown in Figure 5(a). It is evident from figure 5(a), the EDS analysis by the presence of constituent elements of Nb_2O_5-Ag particles such as Nb, O, and Ag can be detected. Figure 5(b) shows the Nb_2O_5-Ag

nanocomposite coating on Ti substrate treated with 5M NaOH and after immersion in SBF was found to be more compact and denser with crack like structure which is uniformly distributed all over the surface. The surface was found to be increased by white precipitates which may be due the formation of apatite layer from the SBF solution. The elemental components as Nb, Ag, Ca, P, O and Mg, C and N are confirmed from the EDS are shown in figure 5(b). The Ca/P ratio is found to be 1.67 result the formation of the direct structural and functional connection between the bone and the surface of load-bearing Ti implant. To form bone-like apatite layer, the Nb_2O_5-Ag nanocomposite coating on Ti substrate is treated in 5M NaOH and was immersed in SBF for 14 days at 36.5^{o}C. Ion exchange with the SBF solution is facilitated as a result, favoring apatite development. Sodium niobate released Na^+ ions into the SBF solution by an ion exchange with the H_3O^+ ions in the SBF when they were added to the solution. [31]. The released Na^+ ions provide more favorable conditions for apatite nucleation on the surface of Ti metals, since they increase the concentration of OH^- which is a component of apatite. The surface covered with sufficient number of negatively charged Nb-OH groups combined selectively with the positively charged calcium (Ca^{2+}) ions [32]. As a result, crystalline calcium phosphate is formed when the negatively charged phosphate (PO43-) ions interact with the positively charged oxide surfaces. Once the apatite nuclei are formed, they can spontaneously grow by consuming the Ca^{2+} and PO_4^{3-} ions in the SBF, as the SBF is already supersaturated with respect to the apatite even under the normal conditions [33, 34].

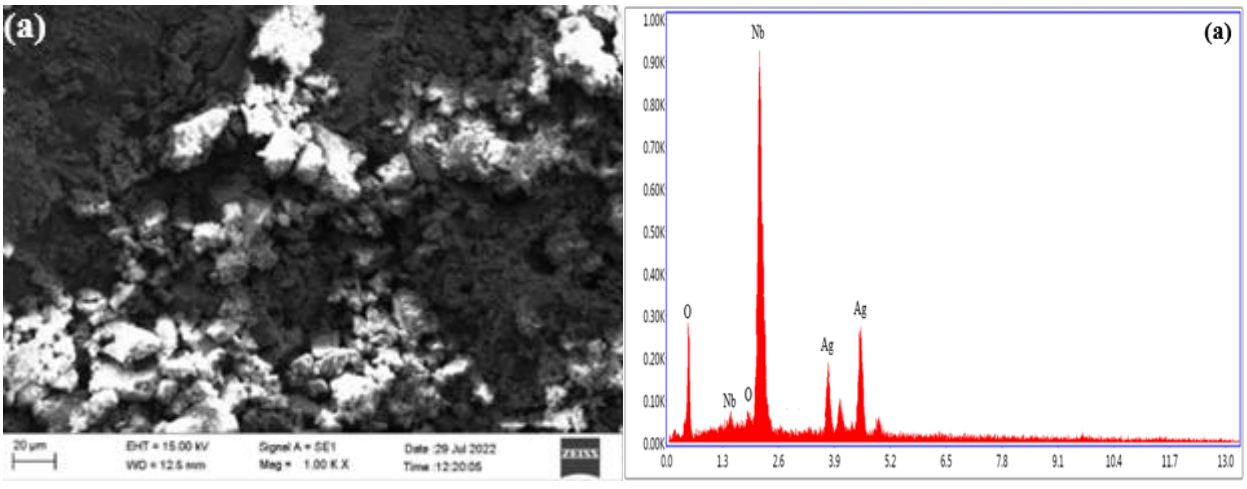

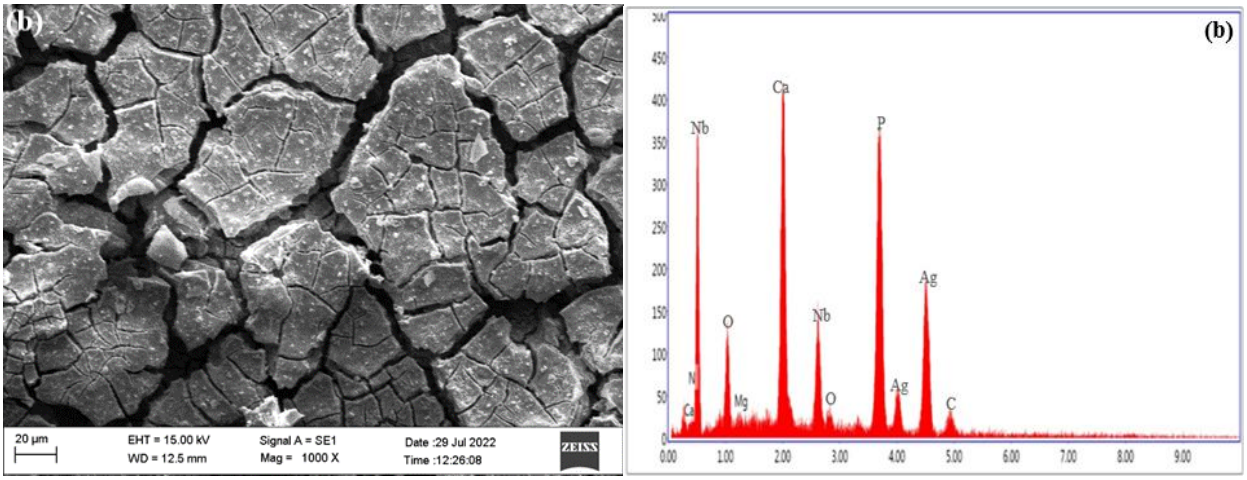

Figure 5: SEM-EDS images of (a) Nb_2O_5-Ag nanocomposite coating with 5M NaOH and (b) Nb_2O_5-Ag nanocomposite coating treated in 5M NaOH and during immersion in SBF at 36.5^oC (pH: 7.4).

Atomic force microscopy (AFM)

AFM with three-dimension images of Nb_2O_5Ag nanocomposite coatings is presented in Figure 6. It is clear that thin coating consists of Nb_2O_5-Ag nanocomposites are observed over the entire surface with a firm layer. The 3- dimensional (3D) AFM image of nanocomposite coating in figure 6(a) is randomly distributed with a maximum value of 8 nm with a root-mean square (RMS) roughness 1.69 nm. It shows the AFM image of the coating before immersion in SBF solution describes surface topography with average diameter of 36 nm. The coatings are found smaller and thinner, showing much smoother surface structures. Figure 6(b) shows the AFM image of the coatings after biomimetic growth in SBF at pH:7.4 and 36.5^o C for 14 days with average diameter of 18 nm. Rmax values got decreased i.e., 0.92 nm after immersion due to the formation of more crystals of apatite i.e., Ca^{2+} and PO_4^{3-} ions on their surface. The thickness of the coating can also be predicted on a single scan by getting the 'z' value i.e., deposited (Z_{coated}) and bare ($Z_{substrate}$) surface of the Ti substrate from the 3D AFM image. It is confirmed from the 3D image of AFM that the thickness of the nanocomposite coating is approximately 80 nm.

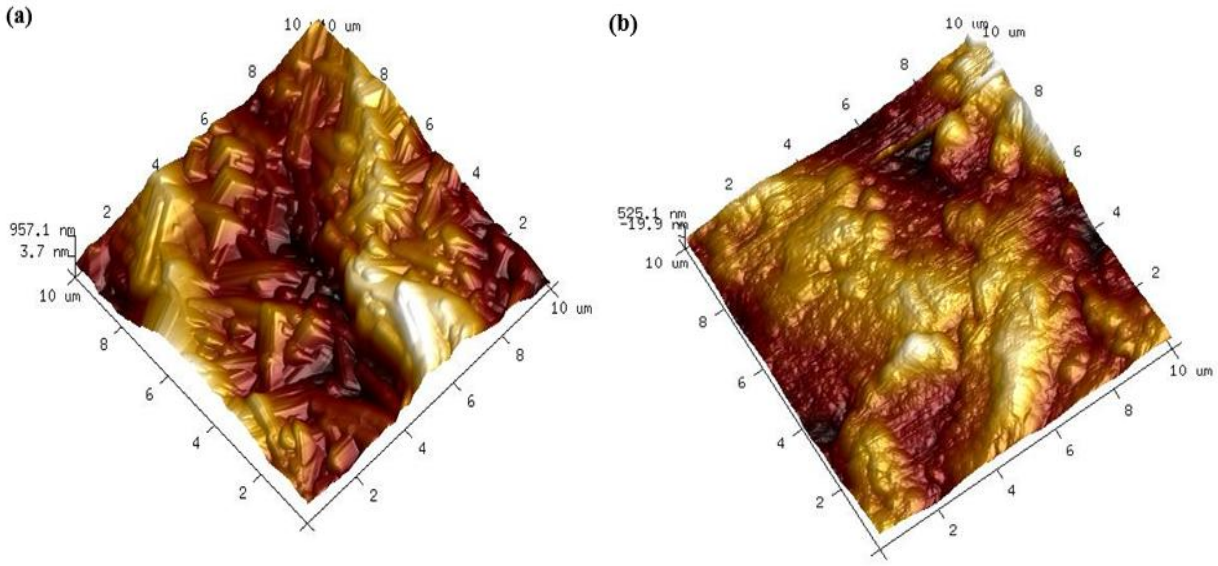

Figure 6: AFM image of (a) Nb_2O_5-Ag nanocomposite coating with 5M NaOH and (b) Nb_2O_5-Ag nanocomposite coating treated in 5M NaOH and during immersion in SBF at 36.5^oC (pH: 7.4).

In vitro antibacterial test

The Nb_2O_5-Ag nanocomposites demonstrate significant antibacterial activity against *Bacillus subtilis, Staphylococcus aureus, Pseudomonas aeruginosa,* and *Escherichia coli*. The antibacterial activities of four different concentrations (0.62, 1.25, 2.5, and 5 mg/mL) of Nb_2O_5-Ag against four bacterial strains, where inhibitory action was studied. In figure 7, the highest inhibitory action of Nb_2O_5-Ag nanocomposite coating was against *Staphylococcus aureus* (Gram positive) and *Escherichia coli* (Gram negative) respectively. The zone of incubation around Nb_2O_5-Ag nanocomposite coatings individual bacterial culture is shown in Figure 8. The clear zone surrounding the sample plates shows the activity of the sample indicating the inhibition of the bacterial culture which gives the efficiency of the antibacterial property of the obtained sample. As the zone of inhibition is high, we can conclude that the obtained Nb_2O_5-Ag nanocomposite coating is an effective antibacterial agent. Antibacterial properties of Nb_2O_5-Ag nanocomposite coatings were highly dependent on the silver content in the nanocomposite coatings. This was especially visible in *Staphylococcus aureus* and *Escherichia coli* which proves that the coating has excellent antibacterial properties.

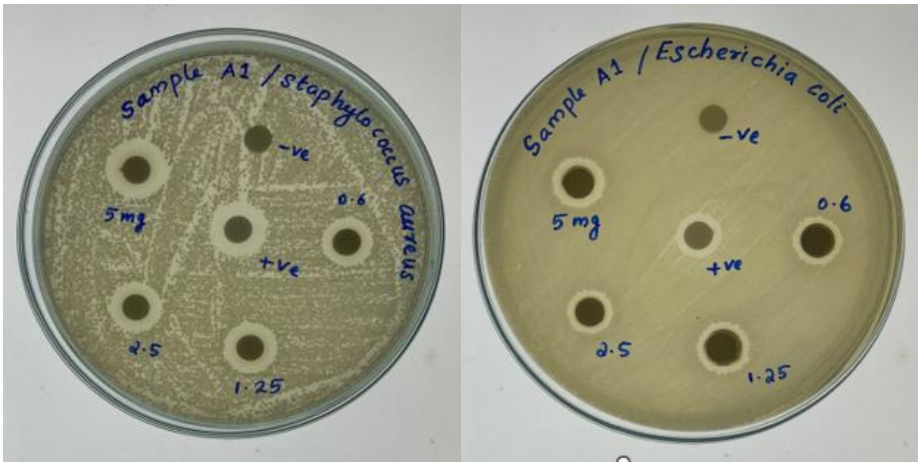

Figure 7: Antibacterial activity of Nb_2O_5-Ag nanocomposite coating on Ti substrate against *Staphylococcus aureus* and *Escherichia coli* respectively.

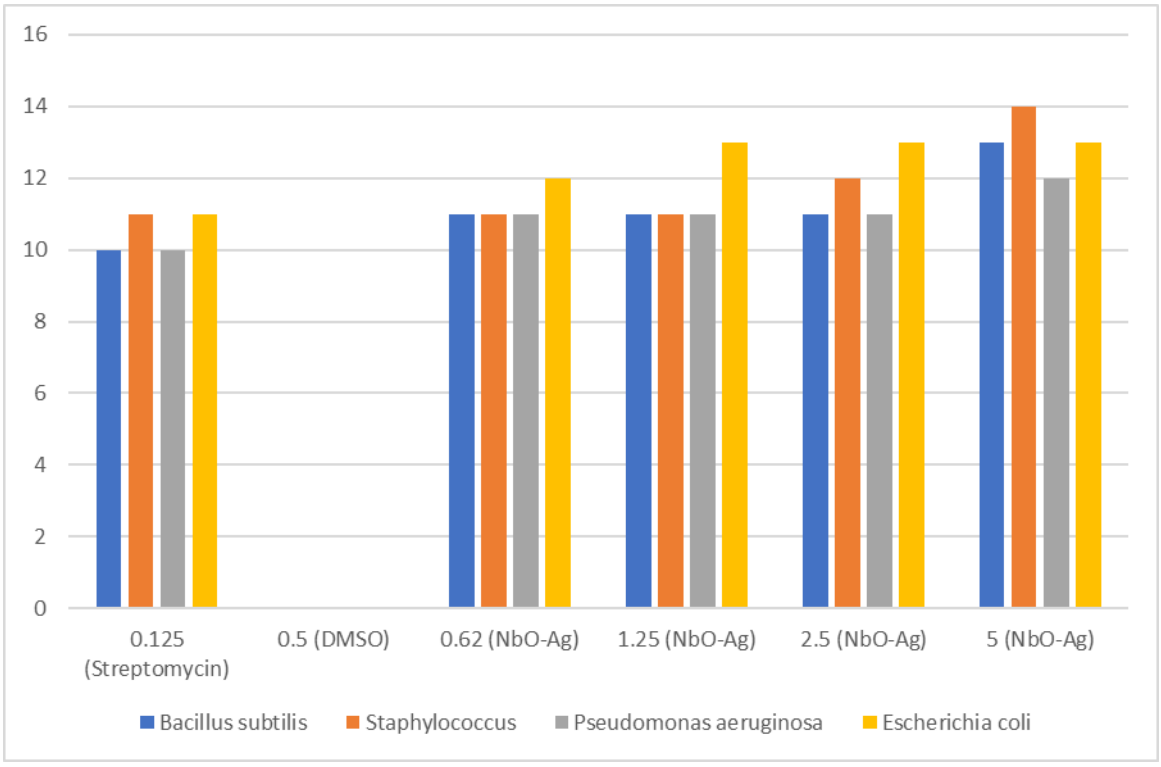

Figure 8: Zone of inhibition on the antibacterial activity of Nb_2O_5 -Ag nanocomposite coating on Ti substrate.

In vitro cytotoxicity test

In this study, the in vitro cytotoxicity of Nb_2O_5 -Ag nanocomposite coating with normal fibroblast cells was evaluated by MTT assay using different concentrations. After in vitro cytotoxicity tests, from figure 9 the cytotoxicity activity in L929 of Nb_2O_5 -Ag nanocomposite coating on Ti substrate was obtained. It was found that fibroblast cells had grown over the surface of the Nb_2O_5 -Ag nanocomposite coating on Ti. The fibroblast retained its spindle shapes and no rupturing was occurred during incubation of the cells with test samples for 24 + 1 hours. Figure 10 illustrated the percentage of viability and MTT assay for varying concentration of test sample in L929 cell line Nb_2O_5 -Ag nanocomposite coating on Ti substrate. Dose dependent reduction in cell viability was observed in cells administered with different concentrations of the sample (6.25-100 µg/ ml). This MTT assay report on L929 cell line reveals that Nb_2O_5 -Ag nanocomposite coating on Ti substrate did not exhibit significant toxic effect on fibroblast cells from 6.25-50 µg/ ml. From figure 11, the cytotoxic activity of Nb_2O_5-Ag nanocomposite coating on Ti substrate was determined. The IC_{50} value of the samples was obtained as 92.02 µg/mL (Figure 11). This in vitro cytotoxicity study provides the evidence that the prepared Nb_2O_5-Ag nanocomposite coating is compatible with normal human fibroblast cells at lower doses i.e., up to 92.02 µg/mL the samples can be applicable and shows faint cytotoxicity at higher doses (above 92.02 µg/mL). From the results, the Nb_2O_5-Ag nanocomposite coatings have negligible cytotoxic effects on healthy human cells to promote bone growth.

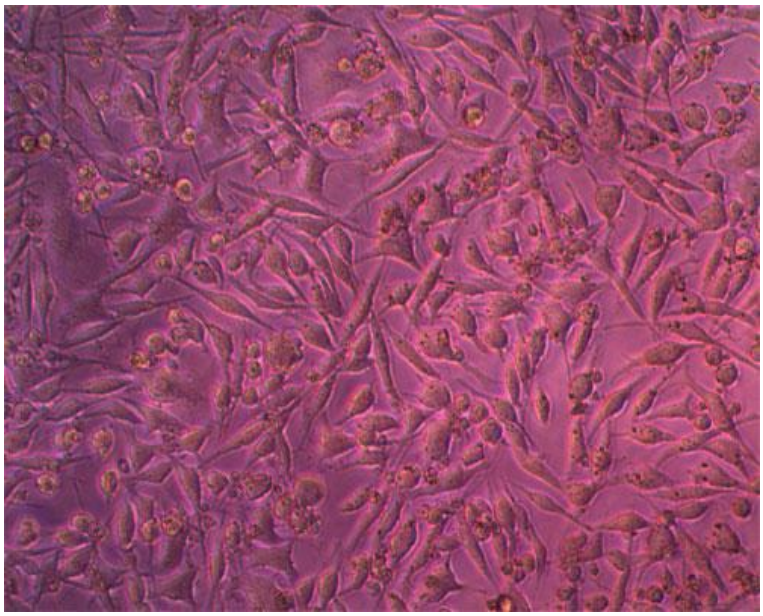

Figure 9: Cytotoxicity activity in L929 of Nb_2O_5 -Ag nanocomposite coating on Ti substrate.

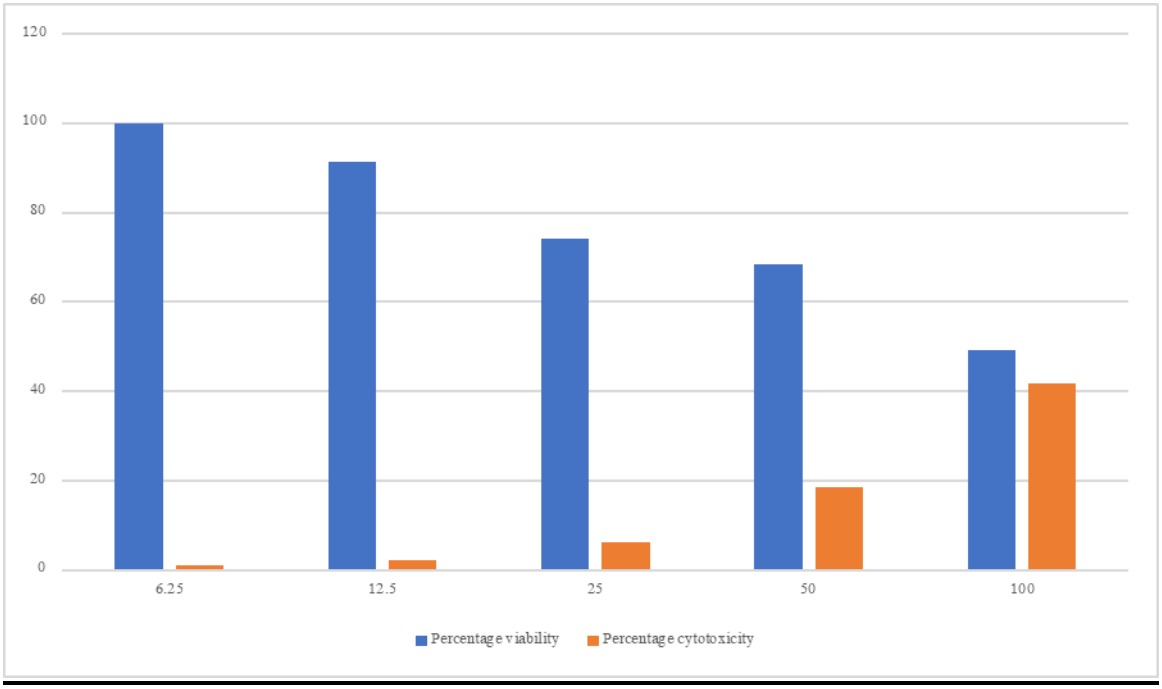

Figure 10: Percentage of viability and MTT assay for varying concentration of test sample on L929 cell line Nb_2O_5 -Ag nanocomposite coating on Ti substrate.

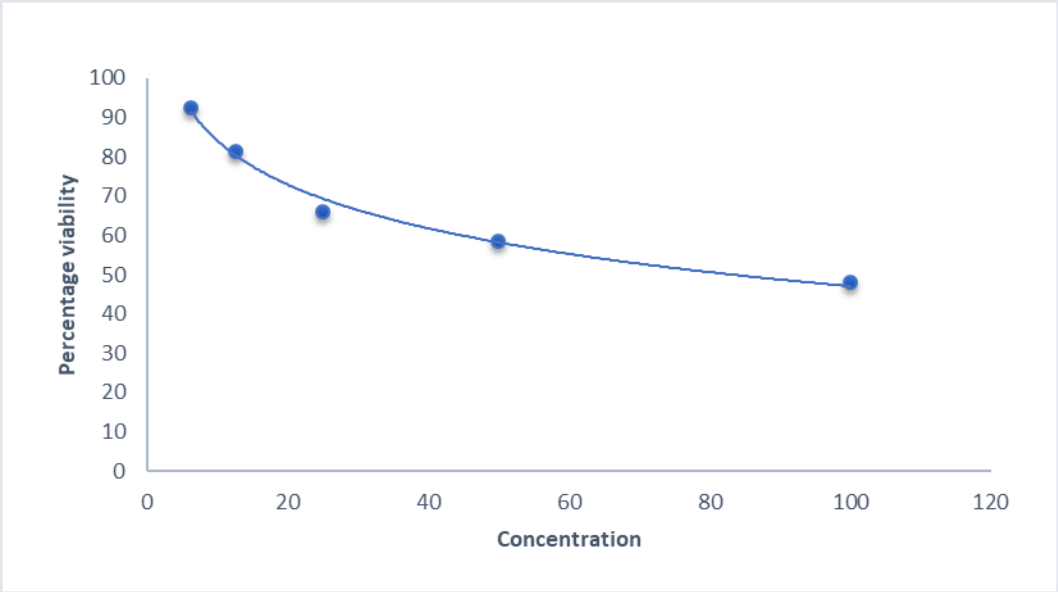

Figure 11: Determination of cytotoxic activity of Nb_2O_5-Ag nanocomposite coating on Ti substrate.

Conclusions

In conclusion, the pulsed electrochemical deposition method was utilized for the Nb_2O_5-Ag nanocomposite coating on an etched Ti substrate. The Nb_2O_5-Ag nanocomposite coating was treated with 5M NaOH to form sodium niobate. The increased apatite forming ability of nanocomposite coated Ti substrate was confirmed by the XRD, FTIR, EIS, CV, SEM-EDS and AFM analyses. The XRD and FTIR analyses confirms the mechanism of Nb_2O_5 and Ag nanoparticles crystallinity and the intensity of sharp bands found to be increased when treated with 5M NaOH and after immersion in SBF for 14 days. These results indicate that Nb_2O_5-Ag nanocomposite coating have the potential for bioactivity, namely bone-like bonding ability when they have a favorable structure such as an orthorhombic crystal phase. There were no detachment or decohesion of the coating indicates it is strongly adhesive and can protect the Ti substrate from the corrosion which was confirmed by CV and EIS annalyses. The SEM-EDS and AFM analysis of Ti substrate after SBF treatment exhibited an appreciable biomimetic growth character with a coating thickness of 80 nm. The EDS shows that the developed nanocomposite coating can enhance the bone growth which was observed 1.67 similar to natural bone in which ossseointegration occurs by forming new apatite crystals in SBF. The corresponding SEM images exhibits the presence of white precipitate of apatite on its surface and also Rmax values

got decreased for Nb_2O_5-Ag nanocomposite coatings treated with 5M NaOH and after immersion in SBF due to the formation of apatite on its surface. Although the mechanism of Nb_2O_5-Ag nanocomposite coating is based on the amount of Ag nanoparticles in the coatings is one of the important factors. A high silver content results in poor biocompatibility while a low silver content results in poor antibacterial properties. The appropriate silver content should be chosen to balance the biocompatibility and antibacterial properties of the nanocomposite coatings. The in vitro antibaterial study shows excellent antibacterial properties due to the co-deposition of silver nanoparticles in niobium pentoxide surface. The cytotoxicity results favors a non-toxic coating material, hence it is suggesting for a future potential-bio interaction between bone and implant for orthopedic and dental applications.

References

[1] Sarrafl M, Ghomi ER, Alipour A, et al. A state-of-the-art review of the fabrication and characteristics of titanium and its alloys for biomedical applications. Bio-Design Manuf. 2021;1(1):1-22.
doi: 10.1007/s42242-021-00170-3.

[2] Trevisan F, Calignano F, Aversa A, et al. Additive manufacturing of titanium alloys in the biomedical field: processes, properties and applications. J Appl Mater. 2017;1(1):1-9. doi: 10.5301/jabfm.5000371.

[3] Naganawa T, Ishihara Y, Iwata T, et al. In vitro biocompatibility of a new titanium-29niobium-13tantalum-4.6zirconium alloy with osteoblast-like MG63 cells. J Periodontol. 2005;75(12):1701-7. doi: 10.1902/jop.2004.75.12.1701.

[4] Chen F, Liu X. Advancing biomaterials of human origin for tissue engineering. Prog Polym Sci. 2016;53: 86-168. doi: 10.1016/j.progpolymsci.2015.02.004.

[5] Mokwa W. Medical implants based on microsystems. Meas Sci Technol. 2007;18(5):47-57. doi. 10.1088/0957-0233/18/5/R01.

[6] Zhao L, Chu PK, Zhang Y, et al. Antibacterial Coatings on Titanium Implants. J Biol Methods. 2009;1(1):470-480. doi.org/10.1002/jbm.b.31463.

[7] Ionita D, Grecu M, Ungureanu C, et al. Modifying the TiAlZr biomaterial surface with coating, for a better anticorrosive and antibacterial performance. Appl Surf Sci. 2011;257(21):9164-9168.
doi.10.1016/j.apsusc.2011.05.125.

[8] Matsuno H, Yokoyama A, Watari F, et al. Biocompatibility and osteogenesis of refractory metal implants, titanium, hafnium, niobium, tantalum and rhenium. Biomaterials. 2001;22(11):1253-1262.
doi: 10.1016/s0142-9612(00)00275-1.

[9] Eisenbarth E, Velten D, Muller M, et al. Biocompatibility of β-stabilizing elements of titanium alloys. Biomaterials. 2004;25(26):5705-5713. doi.10.1016/j.biomaterials.2004.01.021.

[10] Betts AJ, Dowling DP, McConnell M L, et al. The influence of platinum on the performance of silver-platinum anti-bacterial coatings. Mater Design. 2005; 26:217-222. doi.10.1016/J.MATDES.2004.02.006.

[11] Kawashita M, Tsuneyama S, Miyaji F, et al. Antibacterial silver-containing silica glass prepared by sol–gel method. Biomaterials. 2000;21:393-398. doi. 10.1016/s0142-9612(99)00201-x.

[12] Zhao Q, Liu Y, Wang C. Development and evaluation of electroless Ag-PTFE composite coatings with anti-microbial and anti-corrosion properties. Appl Surf Sci. 2005; 252:1620-1627. doi. 10.1016/j.apsusc.2005.02.098.

[13] Pauksch L, Hartmann, Rohnke M, et al. Biocompatibility of silver nanoparticles and silver ions in primary human mesenchymal stem cells and osteoblasts. Acta Biomater. 2014;10(1):439-49. doi. 10.1016/j.actbio.2013.09.037.

[14] Zhao GSSJ. Multiple parameters for the comprehensive evaluation of the susceptibility of Escherichia coli to the silver ion. Biometals. 1988;11(1):27-32. doi: 10.1023/a:1009253223055.

[15] Lu X, Zhao Z, Leng Y. Calcium phosphate crystal growth under controlled atmosphere in electrochemical deposition. J Crystal Growth. 2005; 284:506 -516. doi. 10.1016/j.jcrysgro.2005.07.032.

[16] Yan L, Xiang Y, Yu J, et al. Fabrication of antibacterial and antiwear hydroxyapatite coatings via in situ chitosan-mediated pulse electrochemical deposition. ACS Appl Mater Interfaces. 2017;9(5):5023-5030. doi: 10.1021/acsami.6b15979.

[17] Zhitomirsky I. Electrolytic deposition of niobium oxide films. Mater Lett. 1998; 35:188-193. doi.10.1016/S0167-577X(97)00248-6.

[18] Zhang JM, Lin CJ, Feng ZD, et al. Hydroxyapatite/metal composite coatings prepared by multi-step electrodeposition method. J Mater Sci Letters. 1998; 17:1077-1079.

[19] Lokeshkumar E, Manojkumar P, Saikiran A, et al. Fabrication of Ca and P containing niobium oxide ceramic coatings on niobium by PEO coupled EPD process. Surf Coat Technol. 2021; 416:1-11. doi. 10.1016/j.surfcoat.2021.127161.

[20] Kokubo T, Kushitani H, Sakka S, et al. Solutions able to reproduce in vivo surface-structure changes in bioactive glass-ceramics A-W-G. J Biomed Mater Res 1990;24:721-734. doi.10.1002/jbm.820240607.

[21] Wang YJ, Chen JD, Wei K, et al. Surfactant-assisted synthesis of hydroxyapatite particles. Mater Lett. 2006; 60:3227–3231. doi.10.1016/j.matlet.2006.02.077.

[22] Thankamani V, James J, Arunkumar TV, Dev LMS. Phytochemical screening and antimicrobial activity of Alstonia scholaris flower (L) R.Br. Int J Pharm Res Dev. 2011; 3(4):172-178.

[23] Wayne PA. Performance standards for antimicrobial susceptibility testing, nineteenth informational supplement CLSI document. Clin Labor Std Ins. 2009;1:136-9

[24] Mosmann, T. Rapid Colorimetric Assay for Cellular Growth and Survival: Application to Proliferation and Cytotoxicity Assays. J Immunolog Methods. 1983; 65:55-63. doi. 10.1016/0022-1759(83)90303-4.

[25] Maity D, Bain MK, Bhowmick B, et al. In situ synthesis, characterization, and antimicrobial activity of silver nanoparticles using water soluble polymer. *J Appl Polym Sci*. 2011; 122:2189-2196. doi.10.1002/app.34266.

[26] Canabarro BR, Jardim PM. Effect of synthesis conditions on crystal morphology and layer thickness of nanostructured sodium niobate supported on metallic substrate. *Adv Mater Sci Eng*. 2018; 1:1--10. doi.10.1155/2018/9548340.

[27] Li P, Ohtsuki C, Kokubo T, et al. The role of hydrated silica, titania, and alumina in inducing apatite on implants. Biomed Mater Res. 1994;28:7-15. doi: 10.1002/jbm.820280103.

[28] Devaraj P, Kumari P, Aarti C, et al. Synthesis and characterization of silver nanoparticles using cannonball leaves and their cytotoxicity activity against MCF-7 cell line. J Nanotechnol. 2013; 1:1-5. doi.10.1155/2013/598328.

[29] Moreto JA, Gelamo RV, Pinto MR. New insights of Nb_2O_5 -based coatings on the 316L SS surfaces: enhanced biological responses. J Mater Sci Mater Med. 2021; 32(3):1-25. doi.10.1007/s10856-021-06498-7.

[30] Anjaneyulu U, Priyadarshini B, Stango SAX, Chellappa M, Geetha M, Vijayalakshmi U. Preparation and characterization of sol-gel-derived hydroxyapatite nanoparticles and its coatings on medical grade Ti-6Al-4V alloy for biomedical applications. Mater Technol. 2017;1:1-8.

[31] Liu, X.; Zhao, X.; Fu, R.K.V.; Ho, J.P.Y.; Ding, C.; Chu, P.K. Plasma-treated nanostructured TiO_2 surface supporting biomimetic growth of apatite. Biomaterials. 2005; 26:6143-6150. doi: 10.1016/j.biomaterials.2005.04.035.

[32] Uchida M, Kim HM, Miyaji F, et al. Apatite formation on zirconium metal treated with aqueous NaOH. Biomaterials. 2022; 23:313-317. doi.10.1016/S0142-9612(01)00110-7.

[33] Kim HM, Himeno T, Kawashita M, et al. Surface potential change in bioactive titanium metal during the process of apatite formation in simulated body fluid. J Biomed Mater Res. 2013;67:1305-1309. doi: 10.1002/jbm.a.20039.

[34] Yoshiumi, K.; Tsunehiro, T.; Takuzo, F.; Satohiro, Y. Reaction mechanism in the photoreduction of CO_2 withCH_4 over ZrO_2. *Phys Chem Chem Phys*. 2000; *2*:5302-5307. doi.org/10.1039/B005315.